Solar Energy Materials & Solar Cells 160 (2017) 340–345

Contents lists available at ScienceDirect

Solar Energy Materials & Solar Cells

journal homepage: www.elsevier.com/locate/solmat

Polycrystalline Cu_2O photovoltaic devices incorporating Zn(O,S) window layers

Yulia Tolstova*, Stefan T. Omelchenko, Raymond E. Blackwell, Amanda M. Shing, Harry A. Atwater

California Institute of Technology, Pasadena, CA 91125, USA

ARTICLE INFO

Keywords:
Photovoltaics
Earth-abundant semiconductors
Sputtering
Cuprous oxide
Heterojunction solar cell

ABSTRACT

The tunability of the Zn(O,S) conduction band edge makes it an ideal, earth-abundant heterojunction partner for Cu_2O, whose low electron affinity has limited photovoltaic performance with most other heterojunction candidates. However, to date Cu_2O/Zn(O,S) solar cells have exhibited photocurrents well below the entitled short-circuit current in the detailed balance limit. In this work, we examine the sources of photocurrent loss in Cu_2O/Zn(O,S) solar cells fabricated by sputter deposition of Zn(O,S) on polycrystalline Cu_2O substrates grown by thermal oxidation of Cu foils. X-ray photoelectron spectra reveal that Zn(O,S) deposited at room temperature leads to a thin layer of $ZnSO_4$ at the Zn(O,S)/Cu_2O interface that impedes current collection and limits the short circuit current density to 2 mA/cm^2. Deposition of Zn(O,S) at elevated temperatures decreases the presence of interfacial $ZnSO_4$ and therefore the barrier to photocurrent collection. Optimal photovoltaic performance is achieved at a Zn(O,S) deposition temperature of 100 °C, which enables an increase in the short circuit current density to 5 mA/cm^2, although a small $ZnSO_4$ layer is still present. Deposition at temperatures above 100 °C leads to a reduction in photovoltaic performance. Spectral response measurements indicate the presence of a barrier to photocurrent and exhibit a strong dependence on voltage and light bias, likely due to the photodoping of Zn(O,S) layer.

1. Introduction

Cuprous Oxide (Cu_2O) is an earth-abundant p-type semiconductor with favorable properties and potential for tandem photovoltaic devices. Synthesis of Cu_2O by thermal oxidation of Cu foils in air has produced material with a high visible light absorption coefficient, hole mobilities exceeding 100 cm^2 V^{-1}s^{-1}, and minority carrier diffusion lengths in excess of 10 μm. In addition, Cu_2O is comprised of non-toxic elements and can be cheaply manufactured by oxidizing Cu foils in air. Its large electronic bandgap of 2.1 eV at room temperature makes it a candidate wide bandgap material for a Cu_2O/Si tandem solar cell with a crystalline Si bottom cell. However, the efficiency of Cu_2O photovoltaics remains well below the 20% efficiency of the detailed balance limit for a single junction Cu_2O solar cell [1,2].

Several important challenges have prevented realization of high efficiency Cu_2O devices to date. One stems from the nearly intrinsic and exclusively p-type nature of Cu_2O conductivity, with low hole concentrations dictated by copper vacancy doping and the lack of an n-type doping scheme which has necessitated a heterojunction device architecture. Selection of a suitable heterojunction partner with the correct band alignment has been challenging due to the low electron affinity of Cu_2O (3.2 eV). Much of previous reported work has investigated Cu_2O paired with n-type transparent conducting oxides, such as ZnO. However, the staggered type II band alignment between ZnO and Cu_2O fundamentally limits the V_{oc} and therefore the efficiency. [3,4] In addition, the small heat of formation of Cu_2O (−170.7 kJ/mol) [5] implies that the surface is susceptible to reduction and oxidation. Prior work shows that maintaining stoichiometric Cu_2O at the window/absorber layer interface is important for high efficiency devices [3,6]. It is thus imperative to find a heterojunction window material with an appropriate band offset that allows formation of a stoichiometric Cu_2O interface.

Recently, Ga_2O_3 [7,8] and Zn(O,S) [4,6,9] have emerged as candidate heterojunction window layers for Cu_2O due to their favorable band alignments, and solar cells with open circuit voltages exceeding 1 V have been fabricated for both window layer materials. Currently, the highest efficiency device, which incorporates a polycrystalline Cu_2O absorber and a $Zn_{1-x}Ge_xO$ buffer layer, is 8.1%. [2].

Zn(O,S), which is the focus of this study, is an attractive window layer for Cu_2O photovoltaics due to its tunable conduction and valence

* Corresponding author.
E-mail address: ytolstova@caltech.edu (Y. Tolstova).

http://dx.doi.org/10.1016/j.solmat.2016.10.049
Received 21 July 2016; Received in revised form 14 October 2016; Accepted 29 October 2016
Available online 06 November 2016

band positions as well as the earth-abundance of its constituent elements. The positions of the Zn(O,S) valence and conduction bands are determined by the sulfur to oxygen ratio of the Zn(O,S), so that the band alignment with Cu_2O can be tuned by varying the Zn(O,S) composition. While the tunability of the Zn(O,S) band edge should allow for the fabrication of highly efficient Cu_2O/Zn(O,S) solar cells, the efficiencies of these devices have been limited by low short-circuit current densities and fill factors [6,9]. In this paper we explore the barriers to current transport in Cu_2O/Zn(O,S) devices, and correlate the series resistance to a thin layer of the wide band gap insulator, $ZnSO_4$, which is the most thermodynamically favorable [6] compound in the presence of these elements. We demonstrate that similar to the Zn(O,S)/CIGS interface [10], the Zn(O,S)/Cu_2O interface is prone to $ZnSO_4$ formation, but that deposition of Zn(O,S) at elevated substrate temperatures significantly suppresses $ZnSO_4$ formation, which results in a significant improvement in the current density and the device efficiency. The best results are achieved with a substrate temperature of 100 °C, although even at this temperature some $ZnSO_4$ is still present. We further analyze possible reasons for reduced photovoltaic performance using light and voltage biased external quantum efficiency.

2. Experimental details

Polycrystalline Cu_2O wafers were synthesized from 6N purity Cu foils, which were heated in a quartz tube furnace to 1025 °C under N_2 flow for 4 h. The foils were then oxidized in air for 24 h and cooled under N_2 flow to room temperature. Cu foil thickness was 0.5 mm and the final Cu_2O wafer thickness was approximately 0.8 mm, with typical carrier concentration of 10^{13}–10^{14} cm^{-3} and hole mobilities around 65 $cm^2 V^{-1}s^{-1}$. Cu_2O wafers were cleaned with IPA and loaded into a magnetron sputtering system equipped with several RF sputtering sources and a base pressure of 1.7×10^{-7} Torr. Cu_2O wafers were heated in vacuum to the deposition temperature and annealed for 90 min, or kept under vacuum in the case of the room temperature samples. A Zn(O,S) layer of approximately 45 nm thickness was co-sputtered from ZnO and ZnS targets of 4 N purity at a working pressure of 5 m Torr Ar. Power on the ZnO target was kept at 100 W, and the power on the ZnS target was 85 W. These values were previously determined to yield the highest V_{oc} devices and correspond to a composition of approximately $ZnO_{0.7}S_{0.3}$. After Zn(O,S) deposition, the samples were cooled in vacuum and removed from the chamber. A shadow mask was placed over the samples and a 60 nm ITO layer was then sputtered at 50 W in an Ar atmosphere at a working pressure of 3 mTorr, with no intentional heating. Lastly, an 80 nm Au contact was deposited on the back. Each wafer resulted in 16 solar cells with individual cell area of 0.02 cm^2. These were tested, with the shadow mask, under standard AM 1.5 illumination.

External quantum efficiency measurements were performed using a Xe arc lamp and slit monochromator, and calibrated to a reference Si photodiode with known spectral responsivity. White light bias was provided with a broadband LED. Voltage bias was controlled by a potentiostat. To confirm the composition of the interface, a very thin layer of approximately 1–2 nm of Zn(O,S) was deposited on polycrystalline Cu_2O wafers. The samples were removed from vacuum and transferred to a Kratos Axis Ultra photoelectron spectrometer with base pressure $< 5\times10^{-9}$ Torr. X-ray photoelectron spectroscopy was performed with Al K_α x-rays ($h\upsilon$=1486.7 eV). High resolution scans of the Cu 2p, O 1s, S 2p peaks were acquired at 25 meV step size, 10 eV pass energy, and slot aperture.

3. Results and discussion

3.1. Current-voltage analysis

The solar cell performance was characterized as a function of Zn(O,S) deposition temperature. The current-voltage characteristics

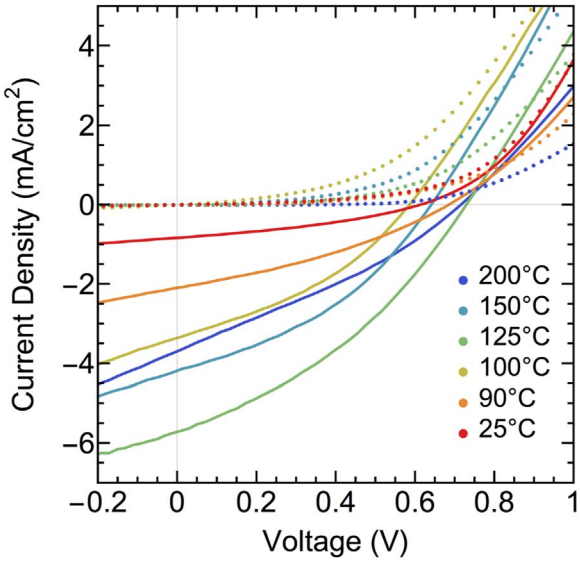

Fig. 1. Current density as a function of voltage in the dark (dashed) and light (solid) for Cu_2O/Zn(O,S) solar cells deposited at different temperatures.

of the most efficient cells for Zn(O,S) deposition at each temperature are shown in Fig. 1 and the overall results are summarized in Table 1. The device deposited at 100 °C has both the highest V_{oc} and J_{sc}. Notably, there is crossover between the dark and light curves for every temperature. Crossover in the J-V characteristics of solar cells has been attributed to an electron barrier in the conduction band which is reduced under illumination and occurs in two general scenarios: 1) under illumination, the window layer is photodoped thereby reducing the potential drop across the window layer and the electron barrier; 2) a high density of electronic defects at the interface are filled with photogenerated carriers under illumination, reducing the electron barrier in the conduction band. [11] The presence of an electron barrier is confirmed by spectral response measurements, as seen in Fig. 2.

The average open circuit voltage, which is correlated to the interface quality, varies from 419 mV at a deposition temperature of 200 °C to a maximum of 724 mV at 100 °C. This suggests that the highest quality Zn(O,S)/Cu_2O interface occurs for a Zn(O,S) deposition temperature of 100 °C. Varying the substrate temperature has a more significant effect on the short circuit current (J_{sc}). The J_{sc} increases from an average of 2.0 mA/cm^2 for devices deposited without intentional substrate heating to a maximum of 5.0 mA/cm^2 for devices deposited at 100 °C, and drops off significantly as the temperature is raised further. In order to understand the apparent barrier to current collection, the dark J-V curve was modeled using the non-ideal diode equation including the impact of series and shunt resistance:

$$I=I_0\left(e^{\frac{q(V-IR_s)}{nkT}}-1\right)+\frac{V-IR_s}{R_{sh}}$$

where I_0,q, n, k, T, R_s and R_{sh} are the dark saturation current, the fundamental electron charge, the ideality factor, Boltzmann constant, temperature and series and shunt resistance, respectively. The fit was obtained using a nonlinear least squares fitting method. As the deposition temperature of Zn(O,S) increases, the series resistance of the device decreases. For reference, through-thickness resistance of the Cu_2O wafer, which was expected to be the largest contribution to series resistance, was measured to be on the order of 800 Ω. For a heterojunction deposited at room temperature, the series resistance is almost an order of magnitude higher, which indicates the presence of a current blocking layer at the junction. At 200 °C, the series resistance of the cell is on the order of the Cu_2O wafer contribution, which suggests the junction resistance has been eliminated. We will analyze this further in

Table 1
Summary of solar cell results.

T dep (°C)	V_{oc} max (mV)	V_{oc} avg (mV)	J_{sc} max (mA/cm^2)	J_{sc} avg (mA/cm^2)	R_s best (Ω)	R_s avg (Ω)	FF max (%)	FF avg (%)	η max (%)	η avg (%)
25	800	704	3.7	2.0	5889	4906	30.3	26.5	0.8	0.4
90	641	615	4.3	4.1	2389	2079	37.4	35.8	1.0	0.9
100	733	724	**5.7**	5.0	2446	2512	35.8	34.7	**1.5**	1.3
125	586	510	3.4	2.9	2146	2118	37.0	33.4	0.7	0.5
150	685	628	2.1	1.9	1329	1324	36.0	34.6	0.5	0.4
200	613	419	0.9	0.8	560	766	37.2	30.9	0.2	0.1

the following sections.

The large series resistance is evident in the low fill factor (FF) observed for all deposition temperatures. The smallest FF is an average of 26.5% for devices deposited at room temperature and increases to a maximum of about 35% for devices deposited at elevated temperature. The fill factor is further limited in the low-current regime by photoshunting, which is apparent from Fig. 1. The efficiency increases from 0.8% for room temperature devices to a maximum of 1.5% for devices deposited at 100 °C, in large part due to the increase in short-circuit current. Ultimately, the efficiency is limited by the low FF and further improvement in the FF of Zn(O,S) devices is needed to increase efficiencies.

3.2. EQE characterization of solar cell deposited at 100 °C

Bias-dependent external quantum efficiency (EQE) measurements were performed in order to further understand the photogenerated collection efficiency and photoshunting observed in the J-V characteristics of Cu_2O/Zn(O,S) solar cells. Fig. 2(a) shows the EQE obtained at different voltage biases without any white light bias. At zero voltage bias, the EQE is close to 60% in the wavelength region from 500 to 570 nm before dropping off at the Cu_2O optical band edge. This indicates that the minority carrier diffusion length in our thermally oxidized Cu_2O is long and does not limit carrier collection far from the depletion region. On the other hand, the EQE in the short wavelength regime (< 500 nm), where carriers are generated close to the Cu_2O/Zn(O,S) junction, is significantly diminished due to recombination at the heterojunction interface.

Fig. 2(b) shows the relative change in EQE with respect to the zero voltage bias. Reverse bias acts to increase the electric field in the depletion region, thereby increasing the band bending and boosting carrier drift. This results in a broadband increase in the EQE for all bias levels. The EQE does not saturate even at large reverse biases indicating the presence of large electronic losses. Similarly, forward

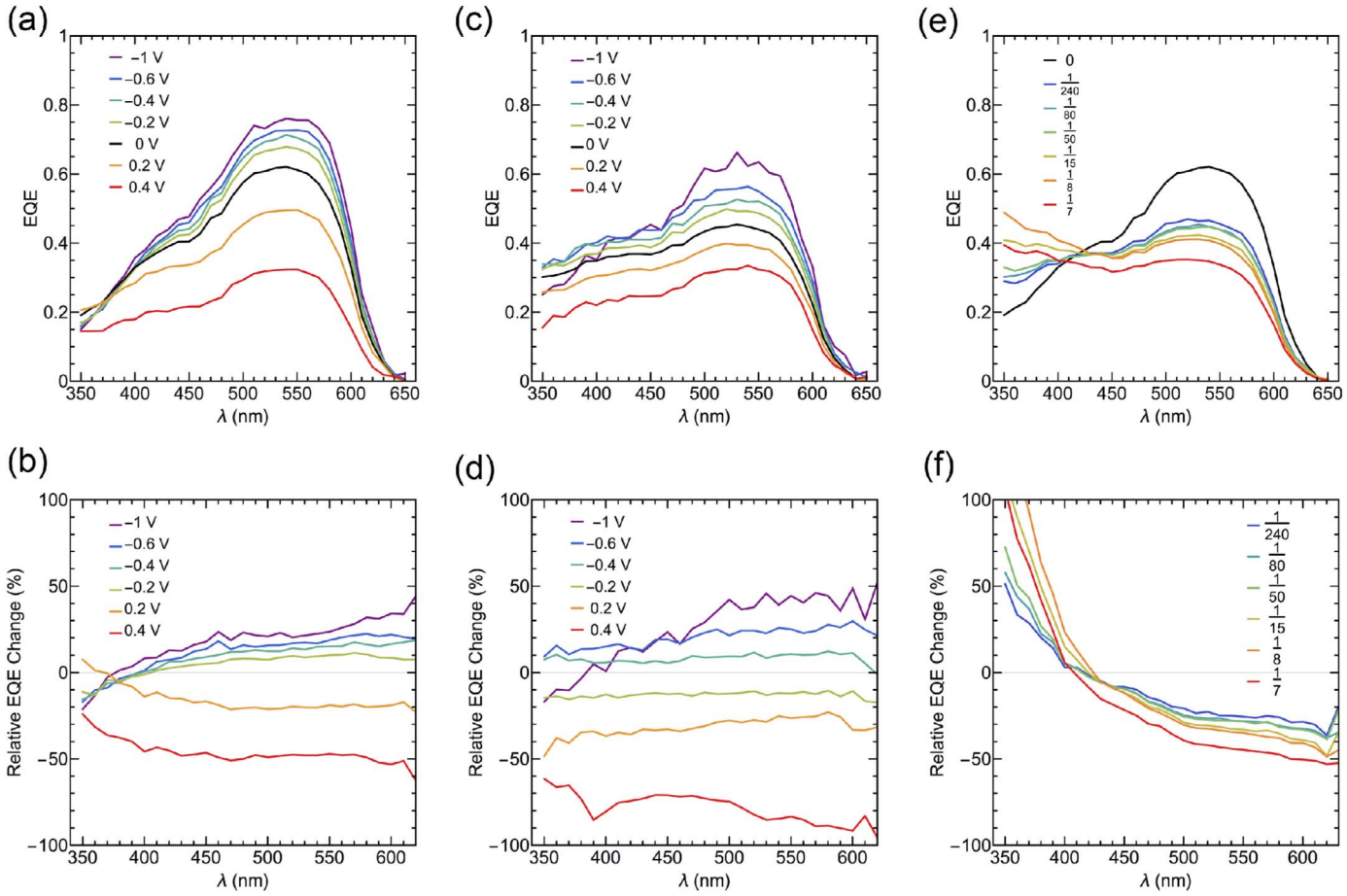

Fig. 2. External quantum efficiency of solar cell deposited at 100 °C (a) with no light bias as a function of applied voltage bias; (b) relative change in EQE compared to zero voltage bias. (c) EQE of same cell with white light illumination of 0.013 suns as a function of applied voltage bias and (d) relative change in EQE compared to short circuit operation under 0.013 sun illumination. (e) Effect of light bias on EQE at short circuit; (f) relative change in EQE as a function of light bias intensity.

bias, leads to a broadband reduction in the EQE at all bias voltages. Fig. 2(c) shows the same experiment performed with white light bias, sourced from a broadband LED, in order to more closely simulate operating conditions. The overall EQE is reduced for wavelengths beyond about 415 nm, which corresponds to the Zn(O,S) band edge, and augmented for shorter wavelengths suggesting strong photodoping of the buffer layer under light bias. The relative change in light-biased EQE with respect to voltage bias is similarly broadband, as shown in Fig. 2(d). Fig. 2(e)–(f) illustrates the effect of light bias intensity on EQE at short circuit conditions, and the strong dependence of EQE response on light illumination intensity suggests that photodoping of the emitter decreases the photocurrent barrier at the heterojunction interface. [11,12].

The integrated EQE without white light bias gives an expected short circuit current of 6.7 mA/cm^2, which is slightly higher than the short circuit current of 5.7 mA/cm^2 measured under standard AM1.5 illumination. However, integrating the EQE corresponding to the largest available illumination level of approximately 0.14 suns gives an expected short circuit current density of 4.3 mA/cm^2, which is significantly lower than the J_{sc} measured using the solar simulator. Extrapolating this trend to an EQE measured at 1 sun illumination would give an even lower expected value of J_{sc}. This confirms the presence of a large barrier to photocurrent in the dark, which is reduced under light illumination by doping the buffer layer. One possible reason for a large photocurrent barrier is the presence of $ZnSO_4$ at the interface between Zn(O,S) and Cu_2O, and we explore this idea in the next section. Another reason for low EQE response compared to the measured J_{sc} is a large density of shunts, which have been seen in solar cells based on thermally oxidized Cu_2O wafers [13].

3.3. XPS characterization of Zn(O,S)/Cu_2O interfaces

X-ray photoelectron spectroscopy (XPS) was used to investigate the chemical composition of the Cu_2O/Zn(O,S) interface and to identify the origin of the current blocking layer. The as-grown surface contains a considerable amount of CuO as evidenced by the satellite peaks between 940 and 945 eV and the shoulder at 935 eV in Fig. 3(a). This CuO layer results from air exposure after the thermal oxidation procedure and is present on all samples. As mentioned previously, CuO at the heterojunction interface has been shown to limit the efficiency of Cu_2O-based solar cells. [3] Two strategies were employed to remove the surface CuO and obtain a stoichiometric Cu_2O interface: substrate annealing in vacuum and reactive sputter deposition. Annealing the Cu_2O substrates at 100 °C in vacuum reduces the amount of CuO present at the surface and CuO is effectively eliminated by annealing at 200 °C. For samples annealed below 200 °C, the reactive removal of CuO during the sputtering of Zn(O,S) is necessary to obtain a stoichiometric surface.

To this end, XPS spectra were also collected from polycrystalline Cu_2O substrates with approximately 1–2 nm thick films of Zn(O,S) deposited at different temperatures in order to examine the stoichiometry of the Cu_2O/Zn(O,S) interface (Fig. 3(b)–(d)). The absence of the shoulder and satellite peaks in Fig. 3(b) confirms the reactive removal of the CuO layer present on the as-grown substrates by deposition of Zn(O,S). In addition, the Cu Auger spectra (see Supplementary information, Fig. 1) did not show any evidence of elemental Cu formation and therefore we conclude that the Cu_2O surface is stoichiometric, which is necessary for the best solar cell performance [3]. The absence of elemental copper and CuO at the interface suggests that the current blocking layer in Cu_2O/Zn(O,S) solar cells originates from another species at the interface. Fig. 3(c) shows the S 2p doublet of the Zn(O,S) film and contains composition information about the sulfur phases that are present at the interface. The main peak position of the $2p_{3/2}$ at 161.8 eV and the $2p_{1/2}$ position at 162.8 eV correspond to ZnS, confirming that the film is primarily zinc oxysulfide. The smaller doublet around 168 eV is attributed to $ZnSO_4$ [14]. It was found previously that $ZnSO_4$ forms primarily at the heterojunction interface [3], with the bulk of the film being the desired zinc oxysulfide phase. Similarly, in CIGS photovoltaics incorporating Zn(O,S), concentrations of $ZnSO_4$ were observed at the Zn(O,S)/CIGS interface that vary with deposition temperature [10]. The Zn(O,S) film deposited at room temperature has the largest amount of zinc sulfate present. The relative sulfate content decreases as the deposition temperature rises and seems to correlate with improved photovoltaic performance up to a deposition temperature of 100 °C. However, above 100 °C both the V_{oc} and the J_{sc} are both significantly reduced relative to the 100 °C case, despite a decrease in $ZnSO_4$ content. Structural changes in the Zn(O,S) do not explain this decrease, as the Zn(O,S) films remain amorphous up to at least 125 °C (see Supplementary information, Fig. 2) but there is a drastic decrease in the J_{sc} and V_{oc} between 100 and 125 °C. The sharp decrease in V_{oc} and J_{sc} could be due in part to a change in the sulfur content of the Zn(O,S) film at elevated temperature, which was observed in CIGS/Zn(O,S) cells [10], and would change the Zn(O,S) band alignment. The V_{oc} decrease at higher deposition temperatures can also indicate a decrease in interface quality, which may be caused by increased interdiffusion. In addition, the lack of CuO on the Cu_2O surface at elevated temperatures could result in changed growth dynamics that alter the interface quality.

In order to check whether the presence of CuO on the surface affected the chemistry of the growing Zn(O,S) film and promoted sulfate formation, a Cu_2O wafer was annealed at 200 °C to remove the CuO layer and then cooled down to 100 °C before depositing Zn(O,S). As shown in Fig. 3(c), the concentration of sulfate in this sample is negligibly different from the sample grown at 100 °C, suggesting that the presence of CuO on the surface does not significantly promote $ZnSO_4$ formation, and that Zn(O,S) deposition temperature is the dominant factor in limiting $ZnSO_4$ at the interface. The oxygen 1s peak in Fig. 3(d) shows presence of the Zn–O bond at 530.4 eV and metal hydroxide at 531.6 eV [15]. The magnitude of the hydroxide peak decreased as the temperature was increased to 100 °C, but was still present. We thus conclude that the decrease in $ZnSO_4$ concentration at the interface is of greater significance to maximizing the short circuit current, but that the remaining hydroxide could still be limiting device performance.

3.4. Structural characterization of Zn(O,S)/Cu_2O interface

Fig. 4(a) shows a bright field cross sectional transmission electron micrograph of the solar cell deposited at 100 °C. The Cu_2O layer root-mean-square surface roughness is approximately 2 nm as measured by AFM and the Zn(O,S) and ITO layers grow conformally. The Pt protective layer on top of ITO is used as a sacrificial layer during focused ion beam sample milling and is not part of the measured device. The thickness of the Zn(O,S) layer is confirmed to be approximately 45 nm and ITO is approximately 55 nm. Fig. 4(b) shows high resolution transmission electron micrographs of the Zn(O,S)/Cu_2O interface, with the inset showing the highest achievable magnification. The Zn(O,S) layer is amorphous with a small amount of nanocrystals, which form due to beam-induced crystallization during the TEM measurement and are not present in the measured solar cells. The Cu_2O surface appears to have very little disorder, and no other phases seem to be present at the interface. The absence of extraneous phases and sharp transition between Zn(O,S) and Cu_2O at the Zn(O,S)/Cu_2O junction are indicative of high interface quality and suggest that other factors limit the device performance.

4. Conclusions

In this work, we investigated the effect of deposition temperature of Zn(O,S) on the performance of Cu_2O/Zn(O,S) photovoltaics. Deposition of Zn(O,S) without intentional substrate heating yields an average short circuit current of only 2 mA/cm^2. The small short circuit

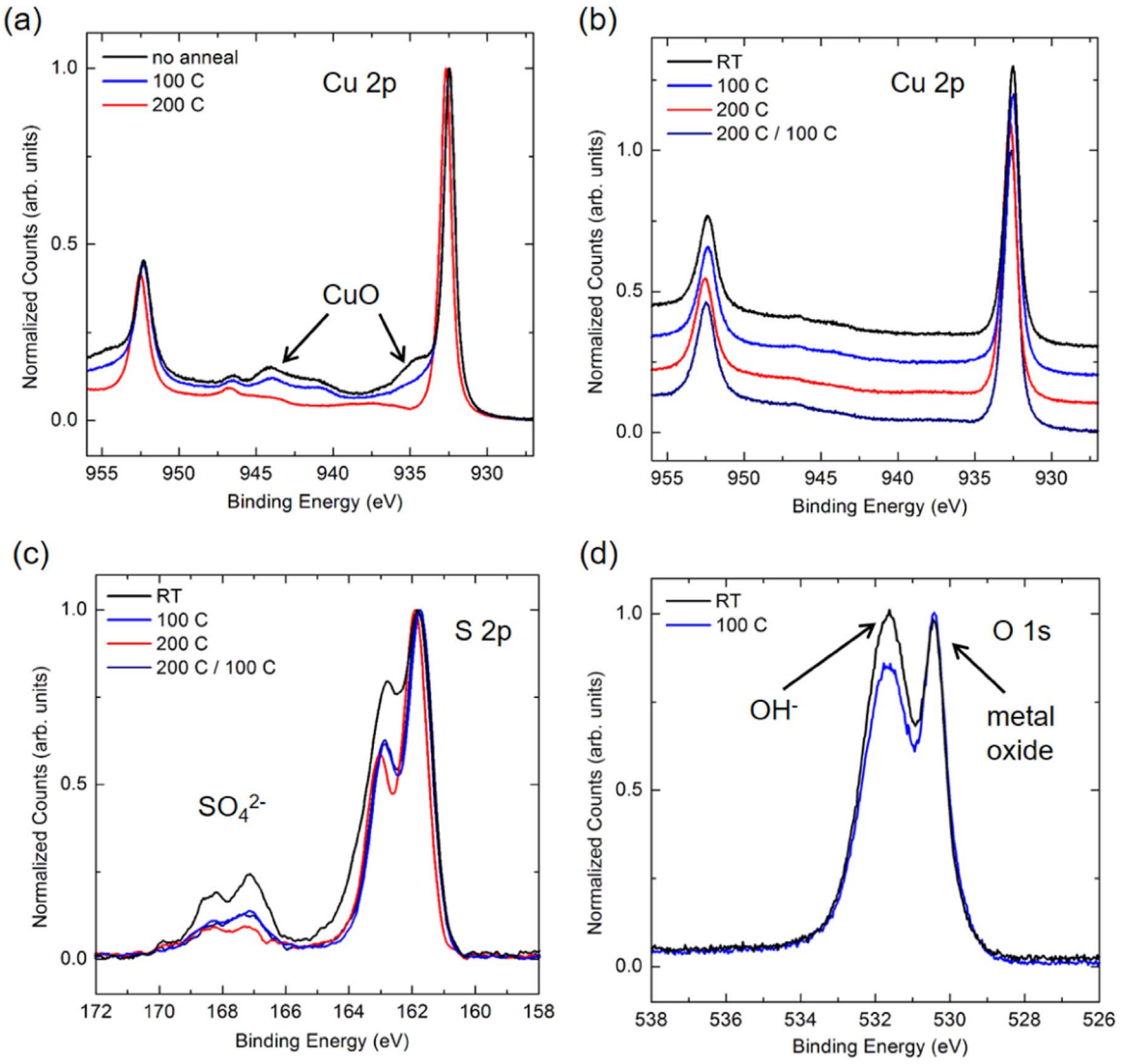

Fig. 3. (a) Cu 2p peaks for a bare Cu_2O wafer annealed in vacuum inside the XPS chamber; (b) Cu 2p peaks; (c) S 2p peaks, and (d) O 1s peaks corresponding to XPS characterization of 1–2 nm Zn(O,S) layers deposited at different temperatures on Cu_2O.

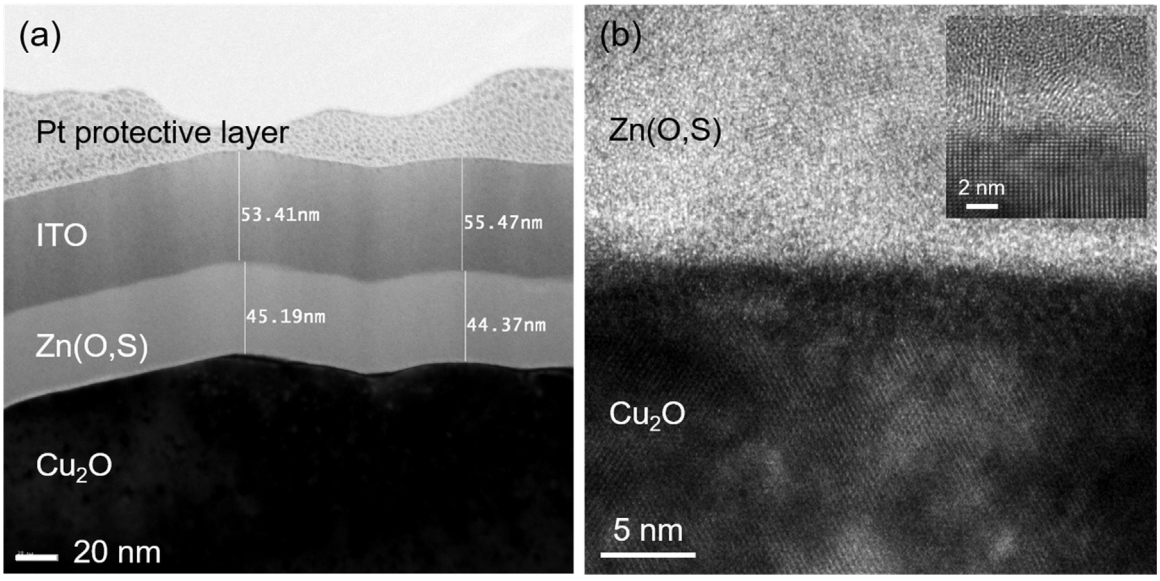

Fig. 4. Transmission electron micrographs of Zn(O,S)/Cu_2O solar cell deposited at 100 C. (a) low resolution bright field image showing film thickness; (b) high resolution image of the Zn(O,S)/Cu_2O interface; (inset) highest magnification.

current density is accompanied by a thin layer of $ZnSO_4$, which we find acts as a barrier to photocurrent. Increasing the substrate temperature results in a substantial short circuit current increase to an average of 5 mA/cm^2 at 100 °C. and is correlated to a suppression of $ZnSO_4$ formation at the Zn(O,S)/Cu_2O interface. However, even in the most efficient cells, $ZnSO_4$ is still present and EQE measurements confirm the presence of a photocurrent barrier and show strong light and voltage bias dependent collection. Depositing Zn(O,S) at temperatures above 100 °C further reduces the presence of $ZnSO_4$ but degrades photovoltaic performance. Further work is needed to address these issues in order to make Zn(O,S) a viable heterojunction window layer for Cu_2O solar cells.

Acknowledgements

The authors gratefully acknowledge support from the Dow Chemical Company under the earth-abundant semiconductor project. This material is based upon work supported in part by the National Science Foundation (NSF) and the Department of Energy (DOE) under NSF CA No. EEC-1041895. Any opinions, findings and conclusions or recommendations expressed in this material are those of the author(s) and do not necessarily reflect those of NSF or DOE. S.T.O. and A.M.S. acknowledge support from the Joint Center for Artificial Photosynthesis, a DOE Energy Innovation Hub, supported through the Office of Science of the U.S. Department of Energy under Award no. DE-SC0004993. XPS data were collected at the Molecular Materials Research Center of the Beckman Institute of the California Institute of Technology. The authors thank Carol Garland at the Caltech Materials Science TEM facility for training and guidance.

Appendix A. Supplementary material

Supplementary data associated with this article can be found in the online version at http://dx.doi.org/10.1016/j.solmat.2016.10.049.

References

[1] L.C. Olsen, F.W. Addis, W. Miller, Experimental and theoretical studies of Cu_2O solar cells, Sol. Cells 7 (1982) 247–279.
[2] T. Minami, Y. Nishi, T. Miyata, Efficiency enhancement using a $Zn_{1-x}Ge_xO$ thin film as an n-type window layer in Cu_2O-based heterojunction solar cells, Appl. Phys. Express 9 (2016) 052301.
[3] S.S. Wilson, J.P. Bosco, Y. Tolstova, D.O. Scanlon, G.W. Watson, H.A. Atwater, Interface stoichiometry control to improve device voltage and modify band alignment in ZnO/Cu_2O heterojunction solar cells, Energy Environ. Sci. 7 (2014) 3606–3610.
[4] R.E. Brandt, M. Young, H.H. Park, A. Dameron, D. Chua, Y.S. Lee, G. Teeter, R.G. Gordon, T. Buonassisi, Band offsets of n-type electron-selective contacts on cuprous oxide (Cu_2O) for photovoltaics, Appl. Phys. Lett. 105 (2014) 263901.
[5] M.W. Chase, Jr., C.A. Davies, J.R. Downey, Jr., D.J. Frurip, R.A. McDonald, A.N. Syverud, NIST-JANAF Thermochemical Tables. ⟨http://kinetics.nist.gov/janaf/janbanr.html⟩, 1986.
[6] S.S. Wilson, Zn-VI/Cu_2O Heterojunctions for Earth-Abundant Photovoltaics, Ph.D. Dissertation, California Institute of Technology. ⟨http://resolver.caltech.edu/CaltechTHESIS:05212015-091546304⟩, 2015.
[7] T. Minami, Y. Nishi, T. Miyata, Heterojunction solar cell with 6% efficiency based on an n-type aluminum–gallium–oxide thin film and p-type sodium-doped Cu_2O sheet, Appl. Phys. Express 8 (2015) 022301.
[8] Y.S. Lee, D. Chua, R.E. Brandt, S.C. Siah, J.V. Li, J.P. Mailoa, S.W. Lee, R.G. Gordon, T. Buonassisi, Atomic layer deposited gallium oxide buffer layer enables 1.2 V open-circuit voltage in cuprous oxide solar cells, Adv. Mater. 26 (2014) 4704–4710.
[9] W. Niu, M. Zhou, Z. Ye, L. Zhu, Photoresponse enhancement of Cu_2O solar cell with sulfur-doped ZnO buffer layer to mediate the interfacial band alignment, Sol. Energy Mater. Sol. Cells 144 (2016) 717–723.
[10] A. Grimm, J. Just, D. Kieven, I. Lauermann, J. Palm, A. Neisser, T. Risson, R. Klenk, Sputtered Zn(O,S) for junction formation in chalcopyrite-based thin film solar cells, Phys. Status Solidi RRL 4 (2010) 109–111.
[11] R. Scheer, H.W. Schock, Chalcogenide Photovoltaics: Physics, Technologies, and Thin Film Devices, Wiley-VCH Verlag GmbH & Co. KGaA, Weinheim, Germany, 2011.
[12] S.S. Hegedus, W.N. Shafarman, Thin-film solar cells: device measurements and analysis, Prog. Photovolt.: Res. Appl. 12 (2004) 155–176.
[13] Y. Tolstova, Cu_2O Heterojunction Photovoltaics, Ph.D. Dissertation, California Institute of Technology. ⟨http://resolver.caltech.edu/CaltechTHESIS:06012016-163813213⟩, 2016.
[14] B.R. Strohmeier, D.M. Hercules, Surface spectroscopic characterization of the interaction between zinc ions and γ-alumina, J. Catal. 86 (1984) 266–279.
[15] NIST X-ray Photoelectron Spectroscopy Database, Version 4.1, NIST, Gaithersburg. ⟨http://srdata.nist.gov/xps/⟩, 2012.